Mass Spectrometric and Photoelectron Spectroscopic Studies of Zirconium Oxide Molecular and Cluster Anions

Owen C. Thomas,[1] Shoujun Xu,[1] T. P. Lippa,[2] and Kit H. Bowen[1, 3]

We present a preliminary report on our mass spectrometric and photoelectron spectroscopic studies of zirconium oxide molecular and cluster anions using a newly built laser vaporization/time-of-flight/magnetic bottle, negative ion photoelectron spectrometer. This work was motivated in part by evidence which suggests that zirconium dioxide catalyzes the radiolysis of interfacial water. We present our mass spectrometric observations of oxygen-rich zirconium oxide cluster anions and our photoelectron spectra of ZrO^- and ZrO_2^-. From the photoelectron spectrum of ZrO^-, the adiabatic electron affinity of ZrO was determined to be 1.3 ± 0.3 eV, and from this value, the dissociation energy of ZrO^- (into Zr and O^-) was found to be 7.8 ± 0.3 eV. From the photoelectron spectrum of ZrO_2^-, the adiabatic electron affinity of ZrO_2 was determined to be 1.8 ± 0.4 eV.

INTRODUCTION

Because of its unique materials properties, zirconium dioxide (zirconia) finds uses in a variety of technological applications [1–6]. Recently, however, heightened interest has developed in a possible, albeit unintended, consequence of its use in the nuclear power industry. Nuclear fuel rods are typically clad, the world over, in zirconium metal alloys, the surfaces of which rapidly become passivated with zirconia, providing a measure of protection against further corrosion. Very often, these fuel rod assemblies

[1] Department of Chemistry, Johns Hopkins University, Baltimore, Maryland 21218.
[2] Present address: Scientific and Engineering Services, Inc., Burtonsville, Maryland 20866.
[3] To whom correspondence should be addressed.

find themselves immersed in water, either as their coolant while in use or as their storage medium once spent. In either case, after prolonged operation in a reactor, such rods become highly radioactive. To this set of circumstances comes emerging evidence [7-9] that the "electronic properties of ZrO_2 may enhance the radiolysis of interfacial water" [7], producing H_2 and O_2 gases (as well as other reactive and thus corrosive species) at a substantially higher rate than would be anticipated based on the radiolysis of water alone. If this is the case and zirconium oxide is "one of the most effective catalysts for radiolytic production of H_2" [7] as has been proposed, the implications for the storage of nuclear fuel rods are significant. For all of their desirable mechanical and thermal properties during use, zirconium dioxide and thus zirconium may have undesirable properties during long-term storage.

The mechanism by which ZrO_2 may be a "gamma enhancer" is thought by Orlando and Petrik [7-9] to be as follows. Ionizing radiation first promotes electronic excitations (excitons) within the micron-thick zirconia skin of a fuel rod, and these then migrate to within 5–10 nm of the surface. Since the energy of these excitations is ~ 5 eV, and since there are likely to be dissociative excited states of chemisorbed water molecules at ~ 5 eV, a resonant transfer of energy is postulated to occur at the zirconia/water interface, resulting in the efficient decomposition of water to H_2 and other products. The specifics may also depend on finite size topological features and non-stoichiometric defects on the surface playing significant roles.

While additional surface and radiological studies are clearly appropriate for pursuing this problem, it might also be useful to determine how the electronic structure of finite-size aggregates of both stoichiometric and nonstoichiometric zirconium oxide compositions evolve with size. In addition to providing points of comparison for theorists trying to model this phenomenon, such information might also offer a measure of physical insight at the microscopic (embryonic solid state) level. With this in mind, we have recently initiated a study of zirconium oxide molecular and cluster anions using time-of-flight mass spectrometry and pulsed, magnetic bottle, negative-ion photoelectron spectroscopy. Here, we present our first results from these experiments. Once additional data are obtained, we plan to follow this brief report with a comprehensive paper.

EXPERIMENTAL

Anions were generated using a laser vaporization source in which a translating, rotating zirconium metal rod was abalated with 532-nm (2.33 eV) light pulses from a YAG laser, while a pulsed valve admitted

oxygen-doped helium gas into the back of the source. The resulting expansion out the front of the source contained anions, neutrals, and cations. A few centimeters away the anions were extracted perpendicularly into a linear time-of-flight (TOF) mass spectrometer using a Wiley–McLaren grid set. After a 1.5-m flight distance, the path of the anions was crossed with a second pulsed YAG laser beam, this one currently operating at 355 nm (3.49 eV). At this photon/ion interaction point, mass-selected anions were photodetached, resulting in free electrons whose kinetic energies (EKE) are related to the photon energy (hv) and the electron binding energy (EBE) by the relationship,

$$hv = EKE + EBE \qquad (1)$$

The anion/photon interaction spot is also the collection point for our magnetic bottle electron energy analyzer. This consists of a permanent magnet just below the ion/photon interaction spot and a long (~ 2.5-m) solenoid region starting just above the interaction spot and terminating at a multichannel plate detector. The laser vaporization source, the TOF ion extraction optics, and the photodetachment laser pulse are all controlled by appropriate timing electronics. Both the mass spectra and the photoelectron spectra are collected and processed by a digital oscilloscope and a laboratory computer. Our pulsed, magnetic bottle, anion photoelectron spectrometer is similar in design to several which have been described in the literature [10–13]. The primary difference between our apparatus and those cited is that ours does not yet have a momentum decelerator, resulting in an electron energy resolution of ~ 0.3 eV at an EKE of 1.5 eV under the conditions cited in this experiment. While this is sufficient for the present preliminary experiments, we plan to improve the resolution of our apparatus (to ~ 0.03 eV at an EKE of 1.5 eV) by adding a momentum decelerator in the near-future.

RESULTS

In this report, we present, for the first time, the mass spectra of zirconium oxide molecular and nonstiochiometric cluster anions as well as the photoelectron spectra of ZrO^- and ZrO_2^-. Future work will focus on photoelectron spectra of ZrO_3^- and the cluster anion species, utilizing 4.65-eV photons where necessary. Figure 1 shows a TOF mass spectrum of the molecular anions produced under source conditions in which O_2 was present in the helium only in trace amounts. Figure 2 presents a TOF mass spectrum of zirconium oxide cluster anions generated under source conditions in which there was 5% O_2 in helium. Note that the observed cluster
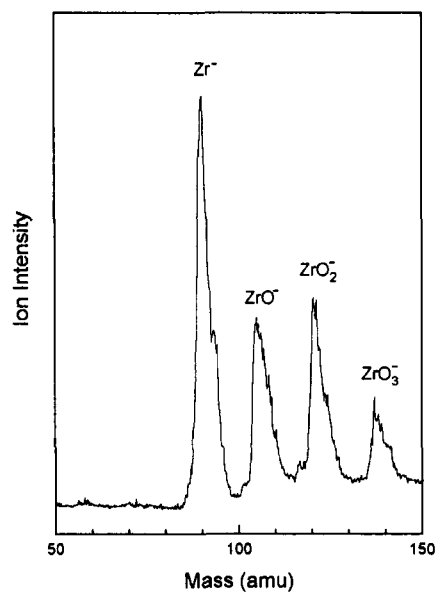
Fig. 1. Mass spectrum showing zirconium oxide molecular anions generated by laser
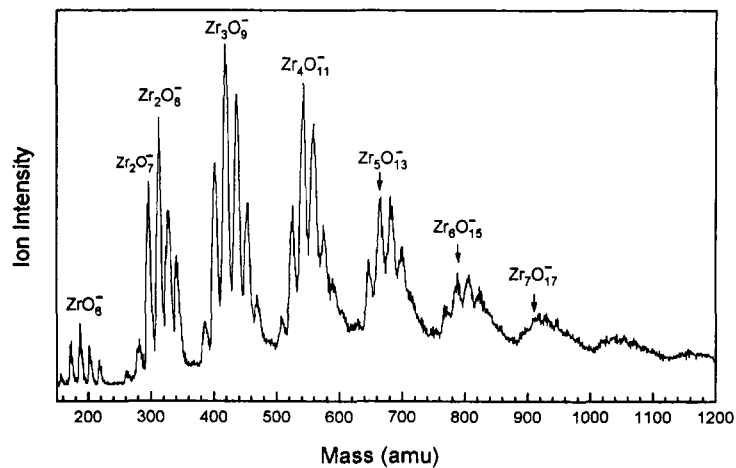vaporization. Zirconium has four significant, naturally occurring isotopes.

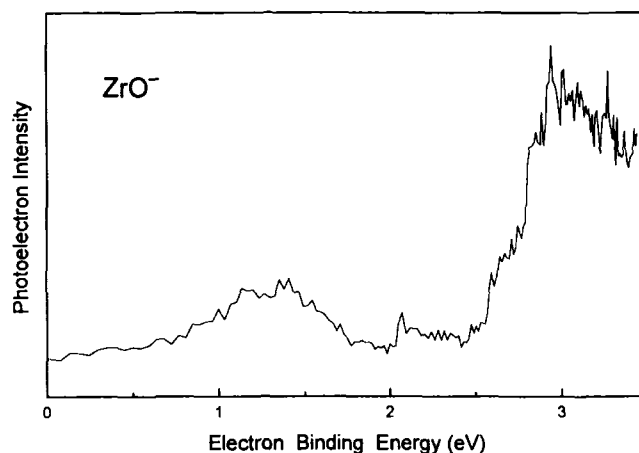**Fig. 2.** Mass spectrum showing zirconium oxide cluster anions generated by laser vaporization.

Fig. 3. Photoelectron spectrum of ZrO⁻ recorded with 3.49-eV photons.

anion species are oxygen-rich. Figure 3 presents our photoelectron spectrum of ZrO⁻. Two unresolved vibronic bands are observed. Figure 4 shows our photoelectron spectrum of ZrO_2^-. Two vibronic bands are observed in this case as well, but with the lower EBE feature exhibiting some spectral structure. Both of these photoelectron spectrum were recorded with 3.49-eV photons as noted above, and both were calibrated against the photoelectron spectrum of the gold atomic anion, Au⁻.
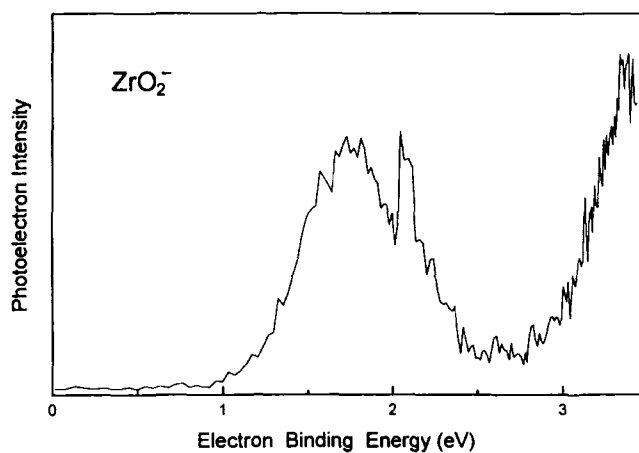

Fig. 4. Photoelectron spectrum of ZrO_2^- recorded with 3.49-eV photons.

ANALYSIS AND DISCUSSION

The most relevant point of comparison is with the mass spectral and anion photoelectron work of Wang *et al.* [14] on titanium oxide molecular and cluster anions. Even though, as Group IVB transition metals, titanium and zirconium share many similiarities, they and their compounds also exhibit differences. These include differences in oxidation states (Ti can be +2, +3, or +4, while Zr is commonly found only as +4) [15], in ligand coordination (Ti binds up to six ligands, while Zr can bind seven) [16], in electron affinities (Ti is 0.2 eV, while Zr is 0.5 eV) [17], and in electronic structure (the ground state of TiO is $^3\Delta$, while that of ZrO is $^1\Sigma$) [18]. A substantial difference appears when one compares the mass spectum of titanium oxide cluster anions presented by Wang *et al.* (Fig. 1 in Ref. 14) with our mass spectrum for zirconium oxide cluster anions in Fig. 2. Wang sees a pattern of cluster anions composed of TiO_2 units along with slightly oxygen-riched species. We do not observe significant intensities of zirconium oxide cluster anions made up of intact ZrO_2 units, at least under the source conditions utilized thus far. The zirconium oxide cluster anion species that we observe are highly oxygen enriched.

Our photoelectron spectrum of ZrO^- (see Fig. 3) implies an adiabatic electron affinity, EA_a, for ZrO of 1.3 ± 0.3 eV. The electronic splitting between its two main bands is ~ 1.5 eV, consistent with spectroscopic measurements on the electronic states of neutral ZrO [19]. In addition, using the following thermochemical cycle,

$$EA_a(ZrO) + D_o(ZrO) = EA(O) + D_0(ZrO^-)$$ (2)

where $EA_a(ZrO)$ is our measured value, $EA(O)$ is the literature value for the electron affinity of the oxygen atom [17], and $D_o(ZrO)$ is the literature value for the dissociation energy of ZrO [20], we have determined $D_0(ZrO^-)$, the dissociation energy of ZrO^- (into the ground atomic states of Zr and O^-) to be 7.8 ± 0.3 eV [21]. By comparison, the EA_a for TiO, as measured by Wang *et al.* [14], is 1.30 ± 0.03 eV, while the splitting between the two main nests of electronic bands in their photoelectron spectrum of TiO^- is also roughly 1.5 eV. Thus, in these respects, the two systems are nearly identical. The main way in which they are different is in the ratios of their low EBE band (integrated) intensities to their higher EBE band (integrated) intensities. In the case of the TiO^- spectrum, its low EBE bands integrate to a substantially higher intensity than its higher EBE bands, while in the case of the ZrO^- spectrum, the opposite is true.

Our photoelectron spectrum of ZrO_2^- (see Fig. 4) implies an EA_a for ZrO_2 of 1.8 ± 0.4 eV. The electronic splitting between its main bands is

again roughly 1.5 eV. By comparison, the EA_a of TiO_2, as measured by Wang et al., is 1.59 ± 0.03 eV, while the splitting between the two main bands in the photoelectron spectrum of TiO_2^- is only a little larger than ~ 1.5 eV. Also, in the cases of these two dioxides, the band intensity ratios are not so greatly different. The photoelectron spectra of TiO_2^- and ZrO_2^- are thus rather similar. The spike-like feature on the high EBE side of the low EBE band in our ZrO_2^- spectrum is reproducuble, but we do not yet understand it. Wang et al. [14] saw a similiar feature on the high EBE side of the low EBE band of their TiO_2^- photoelectron spectrum, which they quite reasonably assigned as vibrational structure. In their case, however, the observed splitting was consistent with the expected 960-cm^{-1} ν_1 mode. In our case, on the other hand, the observed splitting is ~ 1600 cm^{-1}. Since ν_1 is 884 cm^{-1} in ZrO_2 [22, 23], it is difficult to reconcile this feature with vibrational structure. In the future, when we attain a higher resolution, we will return to this issue.

ACKNOWLEDGMENTS

REFERENCES

1. V. A. Loebs, T. W. Haas, and J. S. Solomon (1983). J. Vac. Sci. Technol. A 1, 596.
2. D. P. Taylor, W. C. Simpson, K. Knutsen, M. A. Henderson, and T. M. Orlando (1998). Appl. Surf. Sci. 127, 191.
3. S. Jiang, W. A. Shulze, and G. C. Stange (1997). J. Mater. Chem. 12, 2374.
4. G. Lu, N. Miura, and N. Yamazoe (1997). J. Mater. Chem. 7, 1445.
5. B. Cox (1987). J. Nucl. Mater. 148, 332.
6. V. F. Urbanic, J. E. LeSurf, and J. A. B. Johnson (1973). Corrosion 31, 15.
7. T. M. Orlando, presented at the DOE Environmental Management Science Program Scientific Workshop (Chicago, Illinois, July 27-30, 1998).
8. A. B. Alexandrov, A. Yu. Bychkov, A. I. Vall, N. G. Petrik, and V. M. Sedov (1991). Russ. J. Phys. Chem. 65, 847.
9. T. M. Orlando and N. G. Petrik, Personal private communication (1998).
10. O. Cheshnovsky, S. H. Yang, C. L. Pettiette, M. J. Craycraft, and R. E. Smalley (1987). Rev. Sci. Instrum. 58, 2131.
11. L.-S. Wang, H.-S. Cheng, and J. Fan (1995). J. Chem. Phys. 102, 9480.

12. C.-Y. Cha, G. Gantefor, and W. Eberhardt (1992). *Rev. Sci. Instrum.* **63**, 5661.

13. A. Nakajima, T. Taguwa, K. Hoshino, T. Sugioka, T. Naganuma, F. Ono, K. Watanabe, K. Nakao, Y. Konishi, R. Kishi, and K. Kaya (1993). *Chem. Phys. Lett.* **214**, 22.

14. H. Wu and L.-S. Wang (1997). *J. Chem. Phys.* **107**, 8221.

15. L. Pauling, *General Chemistry* (Dover, New York, 1970).

16. F. A. Cotton and G. Wilkinson, *Advanced Inorganic Chemistry* (Interscience, New York, 1966).

17. H. Hotop and W. C. Lineberger (1975). *J. Phys. Chem. Ref. Data* **4**, 539.

18. K. P. Huber and G. Herzberg, *Molecular Spectra and Molecular Structure, IV. Constants of Diatomic Molecules* (Van Nostrand-Reinhold, New York, 1979).

19. L. A. Kaledin, J. E. McCord, and M. C. Heaven (1995). *J. Mol. Spect.* **174**, 93.

20. H.-P. Loock, B. Simard, S. Wallin, and C. Linton (1998). *J. Chem. Phys.* **109**, 8980.

21. By comparison. $D_0(Zr^+-O) = 7.76 \pm 0.11$ eV. See M. R. Sievers, Y.-M. Chen, and P. B. Armentrout (1996). *J. Chem. Phys.* **105**, 6322.

22. J. L. Margrave, *The Characterization of High-Temperature Vapors* (Wiley, New York, 1967).

23. G. V. Chertihin and L. Andrews (1995). *J. Chem. Phys.* **99**, 6356.